

See discussions, stats, and author profiles for this publication at: <https://www.researchgate.net/publication/303864156>

# The TICTOP nozzle — a new nozzle contouring concept

Conference Paper · May 2016

---

CITATIONS

0

---

READS

410

3 authors, including:



**Manuel Frey**

ArianeGroup, Ottobrunn, Germany

**47** PUBLICATIONS **553** CITATIONS

[SEE PROFILE](#)



**Konrad Makowka**

Airbus Safran Launchers

**8** PUBLICATIONS **4** CITATIONS

[SEE PROFILE](#)

# The TICTOP nozzle — a new nozzle contouring concept

Manuel Frey<sup>(1)</sup>, Konrad Makowka<sup>(1)</sup> and Thomas Aichner<sup>(1)</sup>

<sup>(1)</sup>Airbus Defence and Space, 82024 Taufkirchen, Germany, manuel.frey@airbus.com

**KEYWORDS:** propulsion components, nozzle, flow separation, side-loads

## ABSTRACT

Currently, mainly two types of nozzle contouring methods are applied in space propulsion: The truncated ideal contour (TIC) and the thrust-optimized parabola (TOP). This article presents a new nozzle contouring method called TICTOP, combining elements of TIC and TOP design. The resulting nozzle is shock-free as the TIC and does not induce restricted shock separation (RSS) leading to excessive side-loads. Simultaneously, it will allow higher nozzle wall exit pressures and hence give a better separation margin than is the case for a TOP. This new nozzle type is therefore especially suited for first stage application in launchers where flow separation and side-loads are design drivers.

## 1. Introduction

The main function of a nozzle is to transform potential energy available in the combustion chamber as high pressure and temperature into kinetic energy at the nozzle exit in order to provide thrust. During the nozzle design process, it is important to be aware of the main design rules for contouring, which will be explained in the following.

In most applications, it is favourable for the launch system if the performance is optimized, resulting in a first design rule:

- I. The specific impulse ( $I_{sp_{vac}}$ ) shall be maximized.

In cases where the nozzle is operated only over a narrow range of ambient pressures, one may replace the vacuum specific impulse by the specific impulse averaged over the experienced ambient pressure. For a given combustion chamber, this first requirement is usually reached

via the nozzle contouring. One of the key parameters in this context is the supersonic area ratio  $\epsilon$  of the nozzle. Other parameters to increase the performance are the nozzle length and the contour angle distribution, both mainly influencing the divergence losses.

An important issue for engines operated at sea-level conditions is flow separation, because it is the origin of dangerous, undesired side-loads: Whenever the flow in a nozzle expands to a pressure lower than approximately 30 % of the ambient pressure  $p_a$ , the boundary layer momentum is not sufficient to overcome the higher ambient pressure; as consequence, the wall-near flow is reversed, and the jet separates from the nozzle wall, see **Figure 1**. For the start-up, this is always the case as the chamber pressure is far below its design value.

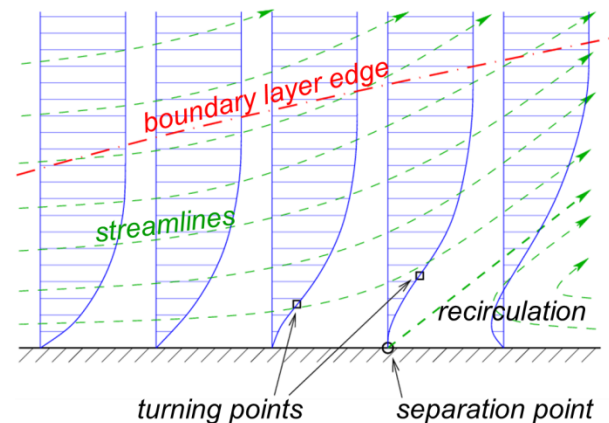


**Figure 1:** Flow separation, general sketch of streamlines and velocity profile [7]

Flow separation in supersonic nozzles is a three-dimensional phenomenon fluctuating in space and time, leading to forces perpendicular to the nozzle axis [7]. The resulting forces are called side-loads and pose a threat to the nozzle, the combustion chamber and their interface as well as for the thrust vector system and even for the payload. Therefore, another important requirement is to reduce side-loads during start-up, as unavoidable separation occurs:

- II. The start-up side-loads shall be minimized.

As the start-up is completed and the rocket engine runs in steady-state, it is usual to require a fully-attached nozzle flow without separation in order to limit side-loads during the flight.

- III. Flow separation during steady-state operation shall be avoided.

Often, there is a conflict between the three design rules, e. g. performance usually requires a high area ratio  $\epsilon$  (rule I), whereas a small area ratio is best suited to avoid flow separation during steady-state (rule III). Hence, a good compromise between the rules has to be found during the contouring process also considering the geometrical envelope that is frequently given as boundary condition.

Currently, mainly two contouring methods are applied for the design of rocket engine nozzles, namely the truncated ideal contour (TIC) and the thrust-optimized parabola (TOP), which shall be briefly outlined in the following.

## 2. Truncated ideal contour (TIC) nozzles

In inviscid flow, it is possible to design so-called ideal contour nozzles that have a uniform exit flow

profile, meaning constant pressure, temperature and velocity over the whole exit plane. Already before the middle of the last century, computational methods to design such contours were available [1], and ideal contours are today still in use for wind tunnel applications. For a given chamber state and throat geometry, the only free design parameter is the design Mach number  $Ma_{des}$ . The higher the design Mach number  $Ma_{des}$ , the higher is the maximum divergence angle and the larger is the nozzle as shown in **Figure 2**.

An ideal contour produces a shock-free flow; its contour is weakly compressive and hence compensates the expansion waves emanating from the throat. At sufficiently high Reynolds numbers, the viscous effects are limited to the thin boundary layer, and the flow remains shock-free also in the viscous case.

For space applications with their restrictive mass requirements, ideal contours are too long and thus too heavy. Furthermore, their nozzle downstream section only contributes little to the thrust because here, the contour is almost parallel to the nozzle axis. Therefore, ideal contours are truncated for space applications, resulting in so-called truncated ideal contours (TIC) [2]. Compared to the ideal contour, the TIC has one more free design parameter in the contouring process, namely the divergent length  $l_{div}$  at which the nozzle is truncated.

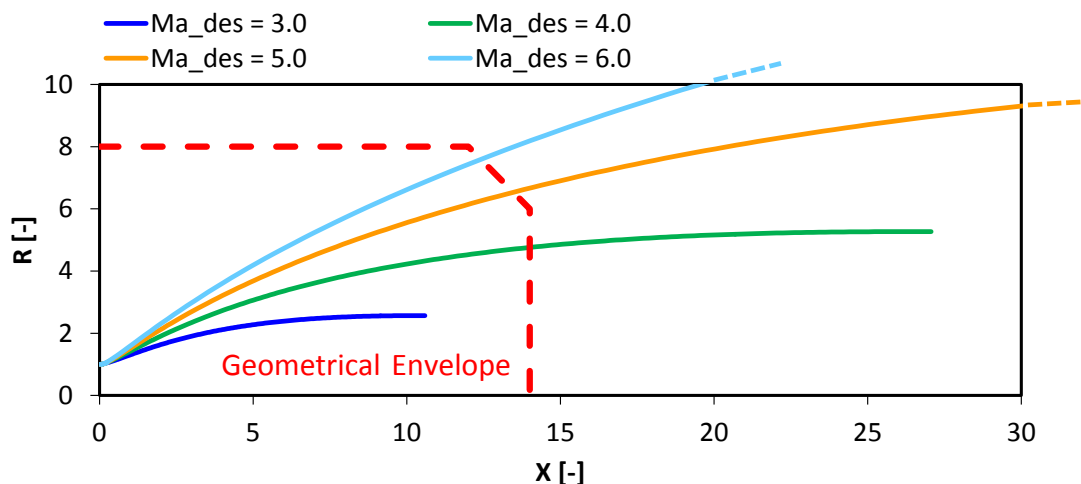


**Figure 2:** Ideal contours with different design Mach numbers  $Ma_{des}$  together with typical geometrical envelope; the necessary truncation is given by the intersection of contour and geometrical envelope

Often, a geometrical envelope is given as boundary condition during the contouring process. In such cases, the geometrical envelope can be drawn into a graph as **Figure 2**. For a given exit point (length and area ratio prescribed), there is exactly one TIC with exactly one exit pressure and specific impulse, hence no free design parameter.

TIC nozzles are widely applied in Russian rocket engines, and also some European and Japanese nozzles use the TIC design.

### 3. Thrust-optimized parabola (TOP) nozzles

The TOP contouring method was proposed by Rao [4] in 1962 as a simplification of his thrust-optimization approach (TOC) published in 1959 [3] that was based on the method of characteristics. With the TOP approach, the nozzle contour was chosen to be a simple skewed parabola. Generally, for a given chamber state and throat geometry, there are four degrees of freedom for a parabola, namely the initial angle  $\theta_i$  and exit angle  $\theta_e$  as well as the nozzle length  $l_{div}$  and area ratio  $\epsilon$ . For a given exit point as is often the case during the contouring process, only the two angles remain as design parameters for a parabola. The thrust optimization is performed by varying these two angles and choosing the nozzle with the highest thrust. Mostly, the optimum is flat, meaning that a moderate variation of e. g.  $1^\circ$  on either angle hardly influences the resulting thrust. Taking into account also the optimization process, there is only one TOP for a given exit point, i. e. there are no free design parameters.

In contrast to the shock-free flow through a TIC, a TOP produces an internal shock originating from the throat region. In order to understand where exactly the internal shock is created, axisymmetric Navier-Stokes simulations of a typical TOP nozzle were performed using the in-house code Rocflam [8]. A Mach number plot is shown in **Figure 3**, where also characteristics (Mach lines) are displayed as indicator for expansion or compression: Diverging characteristics indicate expansion whereas converging characteristics indicate compression. When tracing the last right-running characteristic not being part of the internal shock, one can notice that the internal shock is created in a limited region downstream of the

throat and that consequently, large parts of the supersonic nozzle contour do not contribute to the internal shock at all.

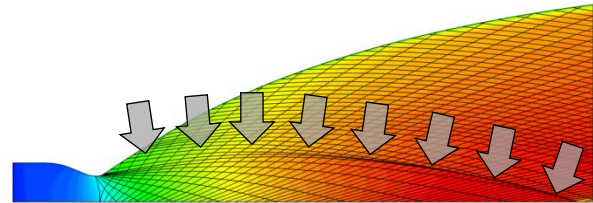


**Figure 3:** Internal shock in a typical thrust-optimized parabola (TOP) nozzle, Mach number isoplot and characteristics (Mach lines); arrows indicate last right-running characteristic contributing to internal shock

The wording "thrust-optimized parabola" seems to imply that a TOP produces the highest possible thrust, i. e. a higher thrust than other nozzles, also than TIC nozzles. However, when comparing a TIC and a TOP through the same exit point, they reach an almost identical vacuum specific impulse  $I_{sp_{vac}}$ . Usually, the difference in  $I_{sp_{vac}}$  is smaller than the prediction accuracy, and in some cases, the TIC produces a higher thrust, in others the TOP. The explanation for this behaviour is that the TOP indeed shows the best performance among all possible skewed parabolas, but not for other contour types as TIC nozzles, that cannot be described as parabolas. From this point of view, the title "thrust-optimized" can be misleading. Both nozzles types TIC and TOP perform similar with respect to the afore-defined requirement I.

In comparison to a TIC nozzle through the same exit point, a TOP usually shows a clearly higher exit pressure. For the typical TOP nozzle shown in **Figure 3**, the wall pressure is 21% higher than for a TIC through the same exit point. This also means that the flow through the TOP will be fully attached when the TIC nozzle still shows flow separation. In other words, the TOP nozzle has a higher margin against flow separation than the TIC through the same exit point, which indicates a better behaviour of the TOP with respect to the requirement III presented in the introduction.

As mentioned before, one of the degrees of freedom of a parabolic nozzle is the nozzle exit angle  $\theta_e$ . This angle governs the nozzle exit pressure; the lower the divergence, the higher the

nozzle exit pressure if all other nozzle parameters are kept constant. During the contouring process, this gives the opportunity to choose an exit angle  $\theta_e$  slightly smaller than the optimum point. Due to the flat  $I_{sp}$  optimum with respect to the exit angle  $\theta_e$ , this will hardly influence the performance, but further increase the nozzle exit pressure, creating even more separation margin.

#### 4. Nozzle types and flow separation

It has been mentioned before that the flow separates from the nozzle wall as soon as the ratio of wall pressure to ambient pressure  $p_w/p_a$  becomes lower than approximately 30 %. This holds true for TIC and TOP nozzles. Usually, the flow separates from the wall and continues as a freejet, which is referred to as free shock separation (FSS), see **Figure 4**. In case the nozzle flow has an internal shock, a second separation pattern can occur. This second separation pattern is characterized by flow reattachment to the wall downstream of the initial separation point, thereby forming a closed recirculation bubble.

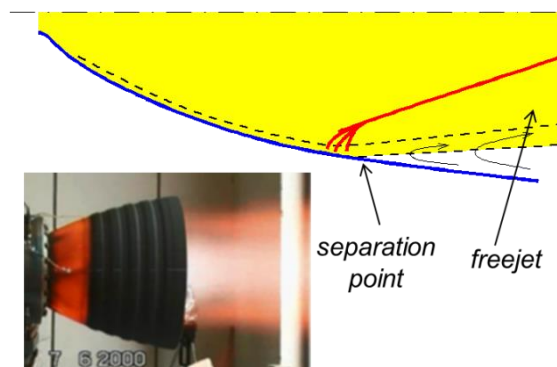


**Figure 4:** Free shock separation (FSS), typical flow-field

This separation pattern only occurs for certain intermediate pressure ratios and is called restricted shock separation (RSS) [6], [7]. Unfortunately, the transition between FSS and RSS as well as vice versa are known to produce very high side-loads [5], [6]. Therefore it is advantageous from a side-loads point of view to choose a nozzle without internal shock, as is the case for a TIC nozzle. Consequently, a TIC nozzle fulfils requirement II better than a TOP nozzle.

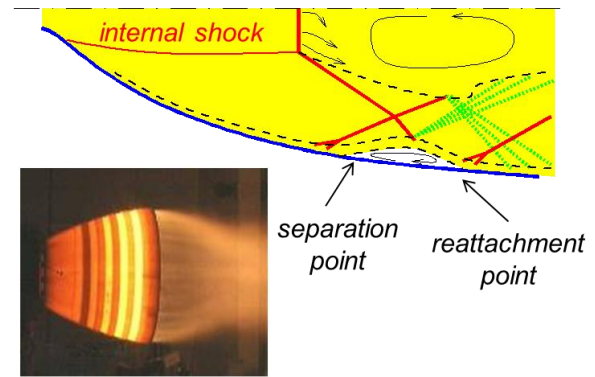


**Figure 5:** Restricted shock separation (RSS), typical flow-field [7]

#### 5. The TICTOP concept

The question is now whether it is possible to design a nozzle combining the good side-load properties of a TIC and the high nozzle exit pressure and better separation margin of a TOP. An approach to do so is the new TICTOP approach presented in this article, which is inspired by **Figure 3**: In a TOP, only a small part of the nozzle contour contributes to the internal shock. The idea is to choose a TIC contour only for this first part of the nozzle and then switch to a parabola downstream as shown in **Figure 6**. The ideal contour in the vicinity of the throat ensures a shock-free flow, and the subsequent parabola can be chosen in a way that the exit pressure is sufficiently high. The transition between the two profiles has to be smooth, there must be no discontinuity in angle (first contour derivative) that could cause a shock. A discontinuity however cannot be avoided in the curvature (second contour derivative).

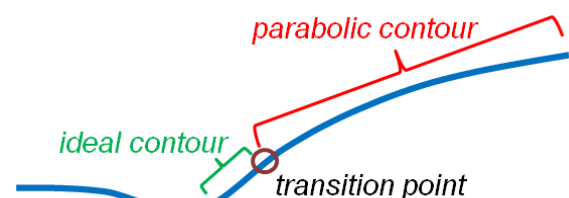


**Figure 6:** The TICTOP principle consisting of an ideal contour upstream of the transition point and a parabolic contour downstream



It is understood that using such a concept, there will be no internal shock as in a TOP emanating from the throat region. However, at least some compression could be caused by either the transition between the two profiles (TIC and parabola) with the resulting discontinuity in the curvature or by the parabolic contour, which must be compressing if the wall exit pressure shall be high. Therefore, it cannot be assumed a priori that the flow in a TICTOP is generally shock-free. As consequence, the generation of compression waves or shocks must be assessed individually for every TICTOP considered.

Without specifying a nozzle exit point, the TICTOP has five design parameters: The design Mach number of the TIC part  $Ma_{des}$ , the axial position of the transition between the two profiles  $l_{TIC}$ , the nozzle length  $l_{div}$ , the area ratio  $\varepsilon$  and the exit angle  $\theta_e$ . In case the TICTOP shall replace an existing TOP nozzle, the nozzle exit point as well as the exit pressure is given. In this case, the exit angle  $\theta_e$  is varied to reproduce the exit pressure of the TOP nozzle. Consequently, only two free design parameters  $Ma_{des}$  and  $l_{TIC}$  remain. **Table 1** gives an overview about the free design parameters for different nozzle types.

**Table 1:** Number of free design parameters for different nozzle concepts for a prescribed chamber state and throat geometry

	TIC	Parabola	TOP	TICTOP
No exit point prescribed	2	4	2	5
Exit point prescribed	0	2	0	3
TICTOP replacing TOP				2

## 6. Example for a TICTOP design: cold subscale nozzle

In order to explain the detailed procedure when designing a TICTOP nozzle, the design of a subscale cold-gas TICTOP nozzle will be presented in the following. In Refs. [5], [6] and [7], a TOP subscale nozzle "DLRTOP" is described, for which the occurrence of RSS and distinct side-load peaks at the transition between FSS and RSS and vice versa have been experimentally

proven. The flowfield of the DLRTOP is shown in **Figure 7**, combining a Rocflam simulation with an existing Schlieren picture of the plume in underexpanded state taken from Ref. [7].

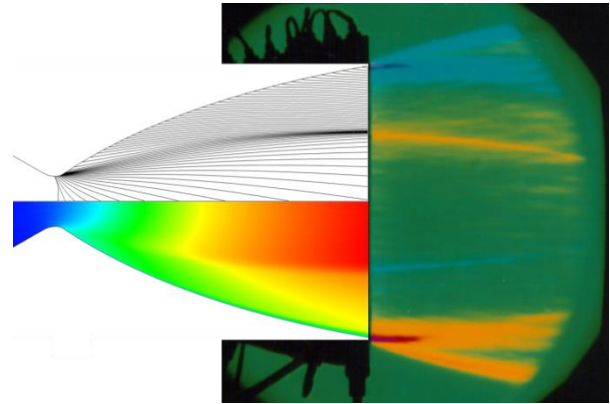


**Figure 7:** Mach number plot and right-running characteristics for the DLRTOP nozzle from Rocflam simulations together with experimental Schlieren pictures (underexpanded plume, Schlieren picture taken from Ref. [7])

The aim is now to design a TICTOP nozzle through the same exit point with a shock-free flow in order to suppress the internal shock and hence the occurrence of RSS and high transitional side-loads.

For the design of the TICTOP nozzle, the exit point and exit pressure of the DLRTOP are prescribed. As described in section 5, two free design parameters exist for such a case, namely the design Mach number of the TIC part  $Ma_{des}$  and the axial position of the transition between the two profiles  $l_{TIC}$ . For each free design parameter four different values were assumed within reasonable limits, leading to a total of sixteen combinations. As a minimum value for  $Ma_{des}$ , the design Mach number for the TIC through the DLRTOP exit point was assumed, whereas for its maximum value, the design Mach number for a TIC with the same initial contour angle  $\theta_i$  as the DLRTOP was chosen. For the axial position of the transition between the two profiles  $l_{TIC}$ , the characteristics of the DLRTOP were evaluated, and the starting point of the first right-running characteristic not in touch with the internal shock was used as reference length.

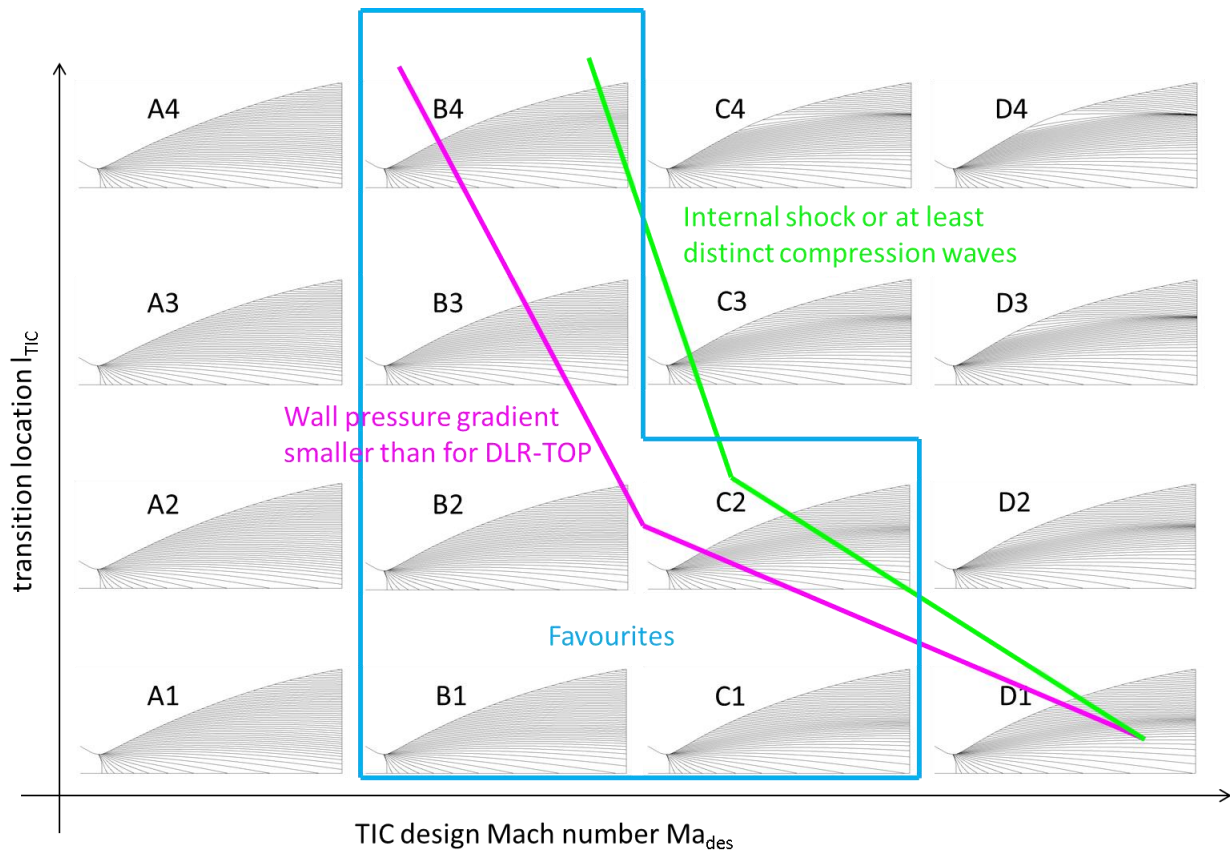


Figure 8: Right-running characteristics evaluated from Rocflam simulations of the sixteen TICTOP nozzles resulting from a variation of  $Ma_{des}$  and  $l_{TIC}$

Two lower values corresponding to 40% and 70% of this reference length and one longer value corresponding to 150%, respectively, were assumed. For each of the sixteen possible combinations of  $Ma_{des}$  and  $l_{TIC}$ , the contour exit angle  $\theta_a$  was varied until the Rocflam recalculation showed a wall exit pressure identical to the DLR-TOP. As nomenclature, letters A to D characterize  $Ma_{des}$  whereas numbers 1 to 4 define  $l_{TIC}$ , leading to sixteen TICTOP nozzles A1 to D4 that are all shown in **Figure 8**.

Rocflam simulations of all sixteen nozzles show only small differences in specific impulse and especially, a performance equal to the DLR-TOP for most contours. However, the upper right three contours in **Figure 8**, namely contours D4, D3 and C4, show a slightly lower  $I_{sp}$  and are therefore disadvantageous in terms of performance. Also, nozzles from the upper right corner of **Figure 8** show an internal shock or at least some undesired compression visible by the convergence of characteristics. This concerns contours C2 to C4

and all contours D (nozzles right of the green line). In these nozzles, due to the internal shock, RSS and undesired high transitional side-loads could occur. A further considered parameter is the wall pressure gradient  $\partial p_w / \partial x$  at the nozzle exit that is known to influence the side-loads occurring during FSS [9]. Higher  $\partial p_w / \partial x$  leads to a reduced fluctuation of the separation location and hence smaller FSS side-loads. In **Figure 8**,  $\partial p_w / \partial x$  increases from the lower left to the upper right, indicating that the FSS side-loads are highest for nozzle A1.

For the DLR-TOP itself,  $\partial p_w / \partial x$  is in the range between B1 and C2, approximately at the magenta line in **Figure 8**. Finding a compromise between a shock-free flow and thus no RSS on the one hand and low FSS side-loads on the other hand, the nozzles B1 to B4 as well as C1 and C2 are favourites. One good choice could be nozzle B1 with its clearly shock-free flow although its wall pressure gradient  $\partial p_w / \partial x$  is slightly lower than the one of the DLR-TOP.

Based on the simulation results, it can be assumed that the TICTOP nozzle B1 and the DLRTOP are similar in terms of functional behaviour (same exit point, same  $I_{sp}$ , same exit pressure  $p_{w,e}$ , almost identical wall pressure gradient at nozzle exit  $\partial p_w / \partial x$ ) with the exception that B1 shows no RSS and hence no high transitional side-loads. A more detailed view on nozzle B1 is taken in **Figure 9**, proving shock-free flow.

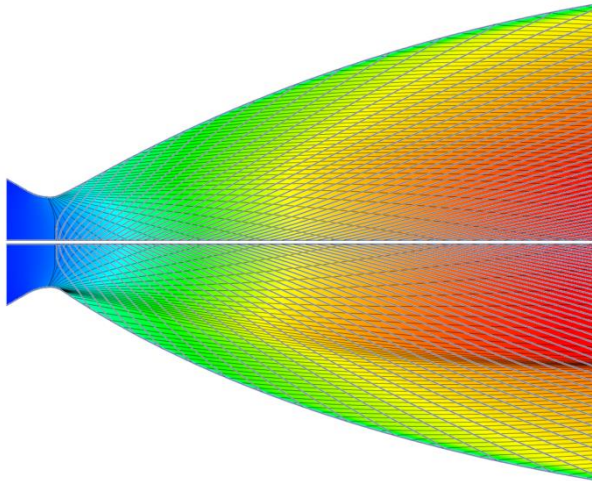


*Figure 9: Mach number plot and characteristics for the TICTOP nozzle B1 (top), clearly showing shock-free flow, compared to the DLRTOP (bottom) with its internal shock*

To show that a shock-free nozzle can not only be designed for cold-gas, but also for hot combustion gases, a TICTOP for a typical  $H_2/O_2$  engine was designed. As in the cold-gas case, the TICTOP shows the same  $I_{sp}$  as a comparable TOP through the same exit point. A Rocflam Mach number plot of the chosen design together with characteristics is shown in **Figure 10**. As can easily be seen, the right-running characteristics do not converge within the nozzle, proving a shock-free flow. Hence, the TICTOP principle appears suited also for typical rocket engine cases.

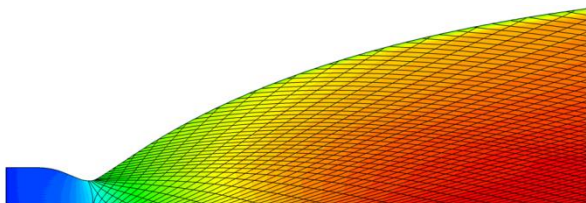


*Figure 10: Rocflam simulation of a TICTOP design for a typical  $H_2/O_2$  engine; Mach number plot and right-running characteristics indicating shock-free flow*

## 7. Conclusion

A new nozzle contouring method has been described, the TICTOP nozzle. It aims at combining the favourable properties of TIC and TOP nozzles, i. e. a shock-free flow with no occurrence of RSS and hence no high transitional side-loads as is the case in the TIC and a high exit pressure providing good margin against steady-state separation as is the case in a TOP. This is reached by combining an ideal contour in the upper part of the nozzle with a parabolic contour in the lower nozzle section. Within this article, a design of a TICTOP has exemplarily been presented for a cold-gas nozzle in detail, showing that it is indeed possible to design shock-free TICTOP nozzles with an  $I_{sp}$  as high as for a TOP. Also for typical launcher applications with hot combustion gases, such design is possible. Hence, in comparison to a TOP, the TICTOP nozzle offers identical functional behaviour, but reduced side-loads.

One open question in the design of a TICTOP nozzle is how much recompression is allowed until the flow really attaches and RSS is formed. In order to clarify this question, cold subscale tests are planned to be performed at DLR Lampoldshausen's P6.2 test facility with two TICTOP contours, one purely shock-free, the other one with some compression and the onset of an internal shock.

## 8. Acknowledgements

Parts of this work have been funded by the German Space Agency DLR within the framework of the research programme TARES, contract number 50 RL 1211.

## 9. REFERENCES

- [1] K. Fölsch: "The Analytical Design of an Axially Symmetric Laval Nozzle for a Parallel and Uniform Jet", Journal of the Aeronautical Sciences, Vol. 16, March 1949
- [2] J. Ahlberg, S. Hamilton, D. Migdal, E. Nilson: Truncated Perfect Nozzles in Optimum Nozzle Design. ARS Journal, Vol. 31, No. 5, May 1961, S. 614-620



- [3] G. V. R. Rao: "Exhaust Nozzle Contour for Optimum Thrust", Jet Propulsion, Vol. No. 6, June 1958
- [4] G. V. R. Rao: "Approximation of Optimum Thrust Nozzle Contour", ARS Journal, Vol. 30 No. 6, June 1960
- [5] M. Frey, R. Stark, H. Ciezki, F. Quessard, W. Kwan: "Subscale Nozzle Testing at the P6.2 Test Stand", AIAA2000-3777
- [6] G. Hagemann, M. Frey, W. Koschel: "Appearance of Restricted Shock Separation in Rocket Nozzles", Journal of Propulsion and Power, Vol. 18, No. 3, May-June 2002
- [7] M. Frey: "Behandlung von Strömungsproblemen in Raketendüsen bei Überexpansion", Shaker Verlag, 2001, ISBN 3-8265-8806-1
- [8] H. Riedmann, J. Görgen, B. Ivancic, K. Makowka, M. Frey: "Numerical simulation of the hot gas side flow and wall heat transfer in CH<sub>4</sub>/O<sub>2</sub> rocket thrust chambers", Space Propulsion 2016 conference, Rome, Italy, May 2016
- [9] R. Schmucker: "Strömungsvorgänge beim Betrieb überexpandierter Düsen chemischer Raketentriebwerke, Teil 2: Seitenkräfte durch unsymmetrische Ablösung", Bericht TB-10, Technische Universität München, 1973